Small Molecule Inhibitors of 8-Oxoguanine DNA Glycosylase-1 (OGG1)

Nathan Donley[1], Pawel Jaruga[2], Erdem Coskun[2], Miral Dizdaroglu[2], Amanda K. McCullough[1], R. Stephen Lloyd[1]*

[1] Oregon Institute of Occupational Health Sciences, Oregon Health and Science University, Portland, Oregon 97239, United States

[2] Biomolecular Measurement Division, National Institute of Standards and Technology, Gaithersburg, Maryland 20899, United States

* E-mail: lloydst@ohsu.edu

ABSTRACT

The DNA base excision repair (BER) pathway, which utilizes DNA glycosylases to initiate repair of specific DNA lesions, is the major pathway for the repair of DNA damage induced by oxidation, alkylation, and deamination. Early results from clinical trials suggest that inhibiting certain enzymes in the BER pathway can be a useful anti-cancer strategy when combined with certain DNA-damaging agents or tumor-specific genetic deficiencies. Despite this general validation of BER enzymes as drug targets, there are many enzymes that function in the BER pathway that have few, if any, specific inhibitors. There is a growing body of evidence that suggests inhibition of 8-oxoguanine DNA glycosylase-1 (OGG1) could be useful as a mono-therapy or in combination therapy to treat certain types of cancer. To identify inhibitors of OGG1, a fluorescence-based screen was developed to analyze OGG1 activity in a high-throughput manner. From a primary screen of ~50,000 molecules, 13 inhibitors were identified, 12 of which were hydrazides or acyl hydrazones. Five inhibitors with an IC_{50} value of less than 1 μM were chosen for further experimentation and verified using two additional biochemical assays. None of the five OGG1 inhibitors reduced DNA binding of OGG1 to a 7,8-dihydro-8-oxoguanine (8-oxo-Gua)–containing substrate but all five inhibited Schiff base formation during OGG1-mediated catalysis. All of these inhibitors displayed a >100-fold selectivity for OGG1 relative to several other DNA glycosylases involved in repair of oxidatively-damaged bases. These inhibitors represent the most potent and selective OGG1 inhibitors identified to date.

INTRODUCTION

The modification of cellular DNA by reactive species, such as free radicals and other oxidizing agents, is a constant challenge to maintaining the fidelity of the nuclear and mitochondrial genomes. Many DNA lesions can be formed in DNA by oxidation.[1] Cells have developed multiple mechanisms to counteract oxidatively-induced DNA damage, including antioxidant strategies, cleansing of the 2'-deoxynucleoside triphosphate (dNTP) pool, and removal of oxidatively-induced lesions from DNA.[1, 2] The base excision repair (BER) pathway, which utilizes DNA glycosylases to initiate repair of specific DNA lesions, is the major pathway for the repair of oxidatively-induced lesions in cellular DNA.[3] Depending on the mechanism of action, DNA glycosylases can either be mono-functional or bi-functional. Mono-functional DNA glycosylases use an activated water nucleophile to catalyze excision of the damaged nucleobase, leaving an intact apurinic/apyrimidinic site (AP site) for AP endonuclease-1 (APE1) to further process. Bi-functional DNA glycosylase/lyases use an amine nucleophile in the enzyme to form a Schiff base intermediate with the DNA, inducing *N*-glycosidic bond cleavage followed by strand scission at the AP site.[4] OGG1 is the human DNA glycosylase responsible for removal of the highly mutagenic 8-oxo-Gua and 2,6-diamino-4-hydroxy-5-formamidopyrimidine (FapyGua) lesions from DNA.[5-7] OGG1 can function as both a mono-functional and bi-functional DNA glycosylase *in vitro*; however, it is still unclear whether one or both functions are utilized *in vivo.*[8]

The BER pathway has recently become a clinically validated drug target for cancer therapy.[9, 10] Inhibitors of BER show promise in two very different treatment protocols. The first is as a single-agent therapy for tumors that have a specific genetic deficiency, usually in another DNA repair pathway. For example, inhibitors of poly (ADP-ribose) polymerase-1 (PARP1) and APE1, two enzymes downstream of the DNA glycosylase step in the BER pathway, can selectively inhibit the growth of cells that have defects in homologous recombination (HR).[11-13] Additionally, cells that lack a functional mismatch repair (MMR) pathway were found to be sensitive to the loss of OGG1 and DNA polymerase β (Pol β), the enzyme responsible for filling the single-nucleotide gap formed during BER.[14] Since genetic deficiencies in the HR and MMR pathways can predispose certain individuals to cancer,[12, 15] mono-therapy with BER inhibitors is a promising treatment option. The second treatment protocol being used in clinical trials is to combine BER inhibitors with chemotherapeutic agents or ionizing radiation (IR) to potentiate the therapeutic effect of these standard-of-care treatments. PARP1 and APE1 inhibitors have been shown to sensitize tumor cells to temozolomide, IR, and multiple antimetabolites.[16, 17] Additionally, preclinical data indicate Pol β inhibitors can also sensitize cells to certain chemotherapies and IR.[9, 18] Despite the validity of the BER pathway as a drug target in cancer treatment, very few DNA glycosylase inhibitors have been identified.

There is a growing body of evidence that inhibition of OGG1 may be useful as a mono-therapy or in combination with DNA damaging agents in the treatment of cancer. Loss of OGG1 function has been shown to sensitize cells to multiple

chemotherapies and IR.[19-21] Additionally, multiple groups have observed that loss of OGG1 sensitized cells to PARP1 inhibitors[22-24] and that overexpression of OGG1 decreased the cytotoxicity of certain platinum drugs.[25] Thus, OGG1 inhibitors have the potential to not only increase the efficacy of certain cancer therapies, but also proactively inhibit potential resistance mechanisms. Further, overexpression of OGG1 reversed RAS-induced growth arrest,[26] indicating that some RAS-driven tumors may be reliant on OGG1 activity in maintaining their neoplastic phenotype and that OGG1 inhibitors may be useful in treating these cancers. Perhaps most interestingly, recent studies have indicated that tumor cells intrinsically generate more oxidatively-induced DNA damage than normal cells and are reliant on pathways that counteract this altered redox potential, opening up a new avenue to target cancer cells while leaving normal cells relatively untouched.[9, 27, 28] It was found that downregulation of Mut T Homolog-1 (MTH1), an enzyme that cleanses the nucleotide pool of free 8-oxodGTP and other modified dNTPs, induced growth arrest and apoptosis in a wide variety of cancer cell lines and had little effect on normal primary cells.[29, 30] Furthermore, MTH1 inhibitors decreased tumor cell growth in a xenograft mouse model.[29] The prominent role that OGG1 plays in repairing oxidatively-induced DNA damage, specifically the 8-oxo-Gua and FapyGua, suggests that OGG1 inhibitors may act very similarly to MTH1 inhibitors to decrease the overall fitness of tumor cells.

In addition to considering OGG1 as a target of small molecule inhibition to augment chemo- and radio-therapeutic strategies, a series of insightful studies have revealed the role of OGG1 in the control of airway inflammation as typified

in asthma pathogenesis (reviewed in[31]). Investigations of the modulation of pulmonary inflammation in *Ogg1*$^{-/-}$ and knocked down mice have been reported using ovalbumin or ragweed pollen extract as pro-inflammatory challenges [32-34]. In these studies, deficiency in OGG1 correlated with significantly less severe responses, including less extensive inflammatory cell infiltration, reduced oxidative damage and decreased activation of Th2-associated genes relative to wild-type animals [32-34]. This suppression in the inflammatory response was correlated with the DNA repair functionality of OGG1, since catalytically dead OGG1 did not elicit the protective response [35]. The molecular basis for this immunosuppression was revealed in a series of publications showing that the release of the 8-oxo-Gua base and its subsequent binding to OGG1 modulates the activation of several GTPases, including RAC1 [33] and KRAS [36], and RHOA [37] and subsequent downstream effectors [33, 36, 38]. These data reveal that the normal release of 8-oxo-Gua is used as a signaling molecule to modulate other cellular processes and responses. In addition, following oxidative stress, OGG1 has also been shown to bind 8-oxo-Gua lesions in promoter sites of NFκB-activated genes, thus promoting rapid transcriptional responses [36, 39]. Overall these data suggest that inhibition of OGG1-initiated 8-oxo-Gua repair and binding could abrogate the severity of allergic airway inflammation.

For these reasons, we set out to identify inhibitors of OGG1. In a previous study, we reduced to practice a screening strategy for inhibitors of the nei endonuclease VIII-like 1 DNA glycosylase (NEIL1) with the goal of expanding this

strategy to screen for inhibitors of other DNA glycosylases.[40] Here, we have adapted this screen for use with OGG1 and have performed the first high-throughput screen for inhibitors of this enzyme. The OGG1 inhibitors identified in this report will be useful as scientific reagents to study OGG1 function and also lay the groundwork for further optimization to identify inhibitors with increased potency for use as therapeutic agents.

RESULTS and DISCUSSION

Development of an OGG1 Inhibitor Screen. Our laboratory recently developed a high-throughput assay to identify inhibitors of human NEIL1.[40] One advantage of this assay is that it can easily be modified to interrogate the activity of any DNA glycosylase that has both glycosylase and associated lyase activities. The OGG1 activity assay utilized a 17-mer oligodeoxynucleotide that contained an 8-oxo-Gua positioned 6 deoxynucleotides downstream of a 5'-TAMRA fluorophore and a complementary DNA strand that contained a 3'-Black Hole Quencher 2 (BHQ2) (Figure 1). While the TAMRA fluorescence signal was quenched in the double-stranded duplex, addition of purified human OGG1 resulted in strand scission and as a result of the lowered melting temperature, the TAMRA-labeled 6-mer was released into solution with its fluorescence no longer quenched (Figure 2a). Consistent with this, addition of increasing amounts of human OGG1 resulted in a dose-dependent increase in TAMRA fluorescence over time (Figure 2b). Furthermore, when an identical reaction was conducted and reaction products were analyzed by size separation through a polyacrylamide gel rather than by

fluorescence, similar dose-response curves were observed, indicating that a measured increase in fluorescence can reliably be used as a readout for the combined glycosylase/lyase activity of OGG1 (Figure 2c). Therefore, inhibitors of OGG1 activity would be expected to result in a weaker fluorescence signal over time compared to a no inhibitor control.

High-throughput Screen for OGG1 Inhibitors. The above assay was miniaturized to a 384-well dish format to screen a ~50,000-molecule Chembridge DIVERset library at a 5 μM concentration. Under the conditions used in this screen, treatment of the 8-oxo-Gua–containing substrate with OGG1 resulted in an ~8-fold enhancement in signal to noise ratio over background. For the 156 plates screened, Z′ values averaged 0.73 with a range of 0.9 to 0.4, indicating a robust screen (Figure 2d). Figure 3 outlines the successive triage strategy to flow from hit to lead identification. Of 49,840 molecules screened, 214 hits were identified as potential OGG1 inhibitors. These hits were rescreened at 8 different concentrations and resynthesized compounds were ordered from Chembridge to test for OGG1 inhibition. This led to the identification of 13 lead compounds that inhibit OGG1 activity with IC_{50} values ranging from 0.29 μM to 7.17 μM.

Hydrazide-containing Molecules Identified as Inhibitors of OGG1. Although it was anticipated that a primary screen of a structurally diverse small-molecule library would identify multiple different inhibitor chemotypes, 12 of the 13 inhibitors identified were either hydrazides or acyl hydrazones. Of the 12 members of this core chemotype, the five most potent OGG1 inhibitors, with IC_{50} values in

the 200–600 nM range, were selected for further study (Table 1). The other eight confirmed inhibitors are listed in Supplemental Table 1.

Four of the identified inhibitors are hydrazides and eight are relatively unstable acyl hydrazones. To test whether the hydrazide form of the acyl hydrazone inhibitors was sufficient to inhibit OGG1, the corresponding hydrazides of O154 and O167 (O8-Cl), and O151 (O151-Hy) were screened for OGG1 inhibition. Both inhibited OGG1 with IC_{50} values less than or equal to their parent molecules (Supplemental Table 1). Since the hydrazide-containing portion of some of the acyl hydrazone compounds appeared sufficient for inhibition, these compounds will be referred to as hydrazide inhibitors for the remainder of this report.

In order to determine whether the hydrazide moiety was necessary for inhibition, the amide form of O151-Hy (O151-Am) was purchased and tested for its inhibitory effect on OGG1. The amide compound had no measureable effect on OGG1 activity at concentrations up to 50 μM (Supplemental Table 1).

A search of the Chembridge library identified a surprisingly high number of hydrazides present in the library (2,325), suggesting that not all hydrazides could inhibit OGG1. We also screened 3 different FDA-approved hydrazides (isoniazid (INH), isocarboxazid (ICD) and nialamide) for OGG1 inhibition and all three of these drugs resulted in little to no inhibition of OGG1 activity with IC_{50} values > 50 μM (Table 1 and Supplemental Table 1). We conclude that some, but not all, hydrazides can inhibit OGG1 function, and that a hydrazide moiety on one of these compounds was necessary for OGG1 inhibition.

Hydrazides Inhibit the Glycosylase and Lyase Activities of OGG1. To verify the results of the fluorescence-based assay, gel-based assays were performed to detect OGG1-mediated strand cleavage of an 8-oxo-Gua–containing substrate at eight different inhibitor concentrations (Figure 4). All five inhibitors showed a dose-dependent inhibition of OGG1 with very similar IC_{50} values to what we observed with the fluorescence-based assay (Figure 4 and Table 1). As expected, the hydrazide non-inhibitor INH showed no inhibition of OGG1 (Figure 4).

There are at least three possibilities that could account for how these molecules inhibit DNA strand cleavage by OGG1. First, they could inhibit only glycosidic bond cleavage, such that AP sites are never generated and strand scission by OGG1 cannot occur. Second, they could be inhibiting only the AP lyase reaction but leave the glycosylase function intact so that AP sites accumulate in the assay. Third, they could inhibit both functions. To examine whether the hydrazide compounds inhibited the AP lyase activity of OGG1, nicking activity was measured on an AP-containing substrate. As shown in Figure 5a, all five inhibitors decreased OGG1-induced cleavage of an AP site compared to the no inhibitor control. Further, the non-inhibitor hydrazides INH and ICD had no effect on this activity. To test whether the glycosylase activity of OGG1 was also inhibited, we utilized a separate mass spectrometry-based assay. This assay used γ-irradiated calf thymus DNA as a substrate and measured the number of free 8-oxo-Gua and FapyGua in solution released by OGG1. This assay had the added advantage of using a more biologically relevant DNA substrate with multiple lesions (total

genomic DNA as opposed to a purified oligodeoxynucleotide containing a single lesion) as well as the ability to measure OGG1 activity on FapyGua in addition to 8-oxo-Gua. As shown in Figure 5b and 5c, incubation with all five OGG1 inhibitors decreased the number of bases released into solution by OGG1 for both the 8-oxo-Gua and FapyGua compared to the no inhibitor control. As expected, INH and ICD resulted in little to no decrease in OGG1-mediated excision of either substrate (Figure 5b and c). We conclude that these five OGG1 inhibitors inhibit both the glycosylase and lyase activities of OGG1.

Hydrazide Inhibitors are Specific to OGG1. It was important to determine whether these OGG1 inhibitors also interfered with the activities of other DNA glycosylases. For these analyses, the OGG1 inhibitors were counter-screened against two other major human DNA glycosylases, NEIL1 and endonuclease III-like (NTH1). Both NEIL1 and NTH1 are able to recognize and cleave the FapyGua.[41-44] Thus, they have some overlapping substrate specificities with OGG1. Additionally, inhibition of the *Escherichia coli* formamidopyrimidine-DNA glycosylase (Fpg) was also analyzed since it has strong activity on 8-oxo-Gua and FapyGua.[45] To test the activity of these three other enzymes, the fluorescence-based activity assay was performed with different substrates (Figure 1 and 2a). All five OGG1 inhibitors displayed little to no inhibition of NEIL1, NTH1 or Fpg with IC_{50} values > 50 μM (Table 1). Furthermore, even with 50 μM inhibitor, there was very little decrease in activity of these enzymes, indicating that IC_{50} values were much greater than 50 μM. This was also the case for the other eight inhibitors identified in our screen (Supplemental Table 1). Therefore, the most potent OGG1

inhibitors showed a >200-fold differential in the inhibition of OGG1 compared to other similar DNA glycosylases.

To confirm these results, we ran the mass spectrometry-based assay with NEIL1 and NTH1. This assay measured excision of the three major substrates from DNA by NEIL1 (4,6-diamino-5-formamidopyrimidine (FapyAde), FapyGua, and 5-hydroxy-5-methylhydantoin (5-OH-5-MeHyd)) and five substrates for NTH1 (FapyAde, FapyGua, 5-OH-5-MeHyd, thymine glycol (ThyGly) and 5-hydroxycytosine (5-OH-Cyt)). Similar to what was observed in the previous assay, all five inhibitors displayed little to no inhibition of NEIL1 for all three substrates analyzed (Supplemental Figure 1); and, despite some modest inhibition of NTH1 on certain substrates, the OGG1 inhibitors also had very little impact on NTH1 activity (Supplemental Figure 2). We conclude that the hydrazide OGG1 inhibitors display strong specificity for OGG1 and have very little inhibitory effect on NEIL1, NTH1, and Fpg.

Hydrazide Inhibitors do not Alter the DNA Substrate. Given that these compounds specifically inhibit the activity of OGG1, they could be acting in one of two ways: They could bind OGG1 and inhibit its action on the DNA substrate or they could bind to the DNA substrate and alter its structure such that OGG1 can no longer recognize it. To test whether these inhibitors could interact with DNA, we first analyzed their ability to intercalate into duplex DNA. Unlike the known DNA intercalating agent ethidium bromide (EtBr), none of the 13 inhibitors identified in the screen showed any evidence of intercalation into a DNA ladder (Supplemental Figure 3a).

It was also possible that these inhibitors could specifically interact with the 8-oxo-Gua or AP sites to inhibit the ability of OGG1 to recognize or excise the lesion. Recent reports have indicated that some aryl hydrazines can interact with the aldehyde on a ring-opened AP site to form a stable complex with the DNA, making the AP site resistant to alkaline-induced strand cleavage [46]. To test whether the OGG1-specific hydrazide inhibitors could function through such a mechanism to inhibit strand cleavage by OGG1, inhibitors were incubated with AP-containing substrate and analyzed whether they protected against NaOH-mediated strand cleavage. While O158 offered modest protection (10%), the other four inhibitors showed no appreciable protection against alkaline-induced strand cleavage (Supplemental Figure 3b). In contrast, the known AP-interacting compound hydralazine gave a 63% protection under the conditions used here. Furthermore, it was found that hydralazine was a poor inhibitor of OGG1 activity, with an IC_{50} > 50 μM (Supplemental Table 1), indicating that reactivity with an AP site was not likely to be the inhibitory mechanism of these molecules.

In a separate experiment, pre-incubation of 8-oxo-Gua– or AP site–containing DNA with each inhibitor for 30 min at 37 °C followed by the addition of Fpg resulted in little to no inhibition of incision (Supplemental Figure 3c). Therefore, we conclude that these hydrazide inhibitors do not intercalate into DNA and do not react with either the 8-oxo-Gua or AP site in such a way that renders them uncleavable by a bi-functional DNA glycosylase.

Mechanism of Action of Hydrazide Inhibitors. The identified inhibitors could be inhibiting OGG1 function by interfering with the ability to bind DNA

substrate or by interfering with catalysis. To test whether these inhibitors affected OGG1 binding to an 8-oxo-Gua or AP site, gel shift assays were performed. As shown in Figure 6a, a gel shift was observed when OGG1 was incubated with an 8-oxo-Gua or AP site, but not with an identical oligodeoxynucleotide that contained a uracil (U). The ability of OGG1 to bind substrate was abrogated in the presence of a known promiscuous inhibitor of DNA-protein interactions aurintricarboxylic acid (ATA).[47] None of the five OGG1 inhibitors had any effect on OGG1 binding to an 8-oxo-Gua substrate and three had no measured effect on OGG1 binding to an AP site (Figure 6a). Interestingly, O151 appeared to increase the affinity of OGG1 for an AP site and incubation with 50 μM O8 inhibitor resulted in an ~40% decrease in AP site binding. However, due to the high concentration used (about 2 logs greater than the IC_{50} value) and the modest decrease in binding, we conclude that the main mechanism of action of O8-induced OGG1 inhibition was not through the interference of OGG1 substrate binding. Therefore, the primary mode of OGG1 inhibition for these five hydrazide inhibitors was not through protein-substrate binding.

To test whether these inhibitors interfere with catalysis, trapping experiments were conducted by carrying out the OGG1 activity assay in the presence of sodium cyanoborohydride. Since the Schiff base intermediate formed during OGG1-mediated strand scission can be trapped under these conditions and the OGG1-DNA complex analyzed on a gel,[48, 49] this assay gives a quantitative measure of the catalytic intermediate formed during the OGG1 reaction. As shown in Figure 6b, OGG1 was trapped on both the 8-oxo-Gua– and AP site–containing

substrates, but not a U-containing substrate in the absence of inhibitor. All five inhibitors decreased trapping on both substrates, while INH had no effect (Figure 6b). Further, trapping assays were performed with titrating doses of the O8 inhibitor. Interestingly, O8 has a calculated T_{50} (concentration of inhibitor needed to reduce borohydride trapping by 50%) of between 0.74 μM and 1.03 μM depending on the substrate (Supplemental Figure 4). These values are slightly higher, but still very close to the calculated IC_{50} value for this inhibitor (Table 1). These data suggest that the primary mode of inhibition for O8, and possibly the other inhibitors, is through the inhibition of Schiff base formation during OGG1 catalysis.

Conclusions. Due to their essential role in the BER pathway of repairing a wide array of DNA lesions from endogenous and exogenous agents, DNA glycosylases are beginning to be evaluated as therapeutic targets in cancer therapy. We have performed the first high throughput screen to identify inhibitors of human OGG1 and have identified a hydrazide/acyl hydrazone inhibitor chemotype that has sub-micromolar potency against OGG1 activity. Interestingly, the hydrazide forms of some of the acyl hydrazone inhibitors were sufficient to inhibit OGG1. This indicates that either the acyl hydrazones break down into the hydrazide form in solution to inhibit OGG1 or that both the acyl hydrazone and hydrazide can inhibit OGG1. Further analyses are underway to understand how this interaction is occurring, as the acyl hydrazones could be useful as prodrugs for therapy.

These inhibitors have little reactivity with DNA and do not inhibit OGG1 substrate interaction. We also found that all of the inhibitors identified are very specific to OGG1. These data were unexpected because many DNA glycosylases have multiple substrates that overlap with other DNA glycosylases. Consistent with this, purine-based inhibitors of NEIL1 were found to be very promiscuous and also inhibited NTH1, OGG1 and Fpg with comparable potencies.[40] Similarly, a recently identified Fpg inhibitor also decreased the activity of other closely related DNA glycosylases.[50] Ongoing experiments of OGG1 co-crystalization with these compounds are anticipated to uncover how these molecules display such high specificity.

The finding that these inhibitors block Schiff base formation during OGG1 catalysis indicates that they mainly function by inhibiting the combined glycosylase/lyase activity of OGG1. Although OGG1 can act as a bi-functional DNA glycosylase, recent studies have suggested that OGG1 also possesses a mono-functional DNA glycosylase activity and it is this activity that is mainly utilized *in vivo.*[8] Interestingly, one of these inhibitors (O151) is a relatively poor inhibitor of Schiff base formation with a T_{50} of ~10 μM (Figure 6b), nearly 20-fold higher than the calculated IC_{50} for this inhibitor (Table 1). This indicates that the abrogation of Schiff base formation is likely not the only mode of inhibition for O151. One possibility is that this inhibitor also interferes with the mono-functional activity of OGG1. In support of this is the observation that, while O151 has the highest IC_{50} value and is the weakest inhibitor of Schiff base formation of the five inhibitors studied here, it is the best inhibitor of the OGG1 glycosylase activity (Figure 5b

and 5c). Although it is tempting to consider these hydrazides as a single family of inhibitors, it is also possible that they may be functioning differently based on subtle changes in structure. Further refinement will be essential to identify OGG1 inhibitors with increased potency and more finely tailored attributes.

METHODS

Reagents. Tris-HCl, Tween-20, EDTA, NaCl, KCl, $MgCl_2$, O8-Cl, O151-Am, isocarboxazid, nialamide, isoniazid, aurintricarboxylic acid, sodium cyanoborohydride, hydralazine HCl, and DTT were purchased from Sigma-Aldrich. Dimethyl sulfoxide (DMSO), urea, acrylamide, bisacrylamide, bovine serum albumin (BSA), glycerol, formamide, ethidium bromide, imidazole, sodium phosphate, and NaOH were purchased from Fisher Scientific. O151-Hy and all the inhibitors identified in the screen were purchased from ChemBridge Corp. 100bp DNA ladder was purchased from New England Biolabs. ProxiPlate-384 Plus F, Black 384-shallow well microplates used in the screen were purchased from Perkin Elmer.

DNA Glycosylases. Fpg and Udg were purchased from New England Biolabs. Human NEIL1, NTH1, and OGG1 were expressed and purified from His-tagged constructs that have been described previously.[40] Briefly, an overnight culture was diluted 1:60 with fresh LB media and shaken at 37°C until OD_{600} reached 0.6. Cultures were cooled to 30°C, IPTG was added to a final 1 mM concentration and cultures were shaken for another three hours at 30°C. Cell pellets were resuspended in 50 mM $NaPO_4$, 300 mM NaCl (buffer) + 25 mM

imidazole, sonicated 4 x 20 sec. bursts with 5 min rests in between, and the cell pellet was spun down. Supernatant was loaded onto a pre-equilibrated Ni-NTA agarose column (Qiagen) and the column was washed extensively with buffer + 50 mM imidazole. Purified protein was eluted in a gradient of 50–500 mM imidazole and glycosylase-containing fractions were combined and dialyzed against 20 mM Tris, 100 mM KCl, 10 mM β-mercaptoethanol, pH 7.0 (dialysis buffer). Samples were equilibrated again in dialysis buffer + 50% glycerol. Purified glycosylase preparations were flash frozen and stored at –80°C.

Oligodeoxynucleotide Substrates. The sequence and lesion information for each substrate used in this report is listed in Figure 1. TAMRA-conjugated oligodeoxynucleotides containing an 8-oxo-Gua or a ThyGly were provided by Dr. Carmelo J. Rizzo (Department of Chemistry, Vanderbilt University, Nashville, TN). All other TAMRA-conjugated, BHQ2-conjugated and unlabeled oligodeoxynucleotides were purchased from Integrated DNA Technologies. Substrate with a mixture of spirodihydantoin (Sp) and guanidinohydantoin (Gh) was generated as described previously.[40] TAMRA-labeled and complement strands were duplexed by heating a 1:1 ratio of each DNA strand in assay buffer (20 mM Tris-HCl, 100 mM KCl, 0.1% BSA, 0.01% Tween-20, pH 7.5) to 65°C for 15 min. The solution was slowly cooled and stored at 4 °C until use. Substrate containing an AP site was generated by treatment of U-containing duplexed DNA with Udg at 37 °C for 2 h.

High-throughput Screen. The fluorescence-based assay outlined in Figure 2a was performed in black, low volume 384-well plates with a final volume

of 10 µL per well. 9 µL of assay buffer (20 mM Tris-HCl, 100 mM KCl, 0.1% BSA, 0.01% Tween-20, pH 7.5) was added to each well, followed by the addition of 1 µL DMSO (control) or 50 µM compound in DMSO. Drug addition and subsequent mixing was performed by an automated robotic system (Sciclone ALH3000 Workstation with the low-volume 384 mandrel array and disposable tips, Perkin Elmer). A total of 20 nL of 25 µM OGG1 in assay buffer + 0.15% Tween was dispensed into each well via a HP D300 digital dispenser (Tecan). Plates were incubated at room temperature (RT) for 5–10 min and then 20 nL of 12.5 µM 8-oxo-Gua–containing substrate (diluted in assay buffer + 0.15% Tween) was dispensed into each well using the same method. The final concentration of each component in the reaction was 5 µM drug, 50 nM enzyme and 25 nM substrate. Plates were incubated for 30 min at 37 °C and TAMRA fluorescence in each well was measured using the Biotek Synergy 4 platereader (Filters = Ex 528/20, Em 600/40. Mirror = Top 570nm with polarizer). Background-subtracted fluorescence values were calculated for each well and any compound that had ≥40 % decrease in fluorescence compared to the no inhibitor control was identified as a hit. Control wells containing just substrate or just substrate + enzyme were used to calculate Z′ values for each plate.

IC_{50} Calculations. Assays to calculate IC_{50} values of OGG1, NEIL1, and NTH1 were fundamentally similar to the high-throughput screen except that the step for the addition of drug differed and a lower enzyme concentration was used. Briefly, 10 µL of assay buffer was added to each well of 384 well dish followed by the addition of 7 different concentrations of drug by the D300 (final drug

concentrations equaled 50, 8.61, 1.48, 0.255, 0.0439, 0.0076, 0.0013 μM). 20 nL of 12.5 μM enzyme (OGG1, NEIL1, or NTH1 diluted in assay buffer + 0.3% Tween) was added to each well and plates were incubated briefly at RT. Subsequently, 20 nL of 12.5 μM substrate (8-oxo-Gua, Sp/Gh, or ThyGly diluted in assay buffer + 0.3% Tween) was added to each well. The final concentration in the reaction was 25 nM enzyme and 25 nM substrate. Plates were incubated at 37 °C for 40 min (OGG1), 5 min (NEIL1), and 10 min (NTH1), followed by the measurement of TAMRA fluorescence. The differing incubation time is due to the different kinetic rates of these enzymes and these times were chosen to analyze incision activity in the linear range. There were three technical replicates per plate and three independent experiments were performed. For NEIL1 and NTH1, all IC_{50} values were >50 μM and could not be calculated. For OGG1, IC_{50} values were calculated using the CurveExpertPro software (http://www.curveexpert.net) with a logistic function sigmoidal curve.

To analyze Fpg activity in the presence of 50 μM drug, Fpg was diluted 1:1000 with assay buffer. 4 μL of diluted enzyme was combined with 1 μL of 500 μM drug and incubated briefly at RT. A total of 5 μL was mixed with 5 μL of 50 nM 8-oxo-Gua substrate and incubated at 37 °C for 10 min followed by TAMRA fluorescence measurement. Final concentration in the reaction equaled 0.032 Units Fpg, 50 μM drug and 25 nM substrate. Three independent experiments were performed. Percent activity compared to the no inhibitor control was calculated in the presence of drug and IC_{50} values were determined to be >50 μM.

Gel-based Cleavage Assay. Gel-based assays were performed by combining 4 µL of 2.5X OGG1 (62.5 nM) with 1 µL 10X inhibitor or buffer. 5 µL 2X substrate (50 nM) was added to bring the final volume to 10 µL. The reaction was incubated 30 min at 37 °C and quenched by the addition of 10 µL formamide and put on ice. Samples were analyzed by electrophoresis on a 15% polyacrylamide gel containing 8 M urea and bands were visualized by a FluorChem M imager (Protein Simple). Band intensities were quantified using the Image Studio Lite Software (LI-COR).

Measurement of Activities of OGG1, NEIL1 and NTH1 by Mass Spectrometry. The enzymatic activities of OGG1, NEIL1 and NTH1 were measured using gas chromatography/isotope-dilution tandem mass spectrometry (GC-MS/MS) and calf thymus DNA samples γ-irradiated at 20 Gy as described.[51, 52] Aliquots of FapyGua-^{13}C,$^{15}N_2$, FapyAde-^{13}C,$^{15}N_2$, 8-oxo-Gua-$^{15}N_5$, 5-OH-Cyt-^{13}C,$^{15}N_2$, ThyGly-d_4, and 5-OH-5-MeHyd-^{13}C,$^{15}N_2$ were added as internal standards to 50 µg of DNA samples. After drying in a SpeedVac, DNA samples were dissolved in 50 µL of an incubation buffer consisting of 50 mM phosphate buffer (pH 7.4), 100 mM KCl, 1 mM EDTA, and 0.1 mM dithiothreitol, and then incubated with 2 µg OGG1, NEIL1, or NTH1 for 1 h at 37 °C without any inhibitor or with 10 µL DMSO alone or with 10 µL of an inhibitor solution in DMSO (10 mM). The final amount of each inhibitor in the incubation buffer was 0.1 µmol. After incubation, 150 µL of cold ethanol were added. The samples were kept at –20 °C for 1 h and then centrifuged with 14000 g for 30 min at 4 °C. The supernatant fractions were separated and ethanol was removed in a SpeedVac under vacuum.

The samples were then frozen in liquid nitrogen and lyophilized overnight. To fully remove DMSO that, if left behind, causes problems for GC-MS/MS analysis, 500 µL water were added to the samples followed by lyophilization overnight. This procedure was repeated twice. Dried samples were derivatized and analyzed by GC-MS/MS as described.[51, 52] For each data point, three independently prepared samples were used.

Gel-shift Assay. All experiments were performed on ice with pre-cooled reagents. These conditions permitted the binding of OGG1 to DNA substrate, but were not permissive for enzymatic cleavage (data not shown and [49]). A total of 4 µL of 2.5X OGG1 (125 nM) was mixed with 1 µL of 10X inhibitor or buffer and incubated on ice 5–10 min. 5 µL 2X substrate (50 nM) was added, mixed and kept on ice for 5 min. The reaction was quenched with 10 µL ice-cold 30% glycerol and loaded onto a pre-cooled 8% native gel containing 30% glycerol. The gel was run at 4°C for 1 h (75 V) and bands were visualized by a FluorChem M imager. Band intensities were quantified using the Image Studio Lite Software.

Sodium Cyanoborohydride Trapping Assay. A total of 4 µL of 2.5X OGG1 (125 nM) was mixed with 1 µL of 10X inhibitor. In a separate tube, 1 µL of freshly prepared 10 mM $NaBH_3CN$ (diluted in H_2O) was mixed with 4 µL of 2.5X substrate (50 nM). Tubes were quickly mixed and the reactions incubated 5–10 min at RT. Reactions were quenched by the addition of SDS loading buffer and heated to 65 °C for 15 min. Samples were run on a 22% SDS-polyacrylamide gel and bands were visualized by a FluorChem M imager. Band intensities were

quantified using the Image Studio Lite Software. T_{50} calculations were performed identically to IC_{50} calculations.

Statistical analysis. The statistical analyses of the data was performed using the GraphPad Prism 6 software (La Jolla, CA, USA) and unpaired, two-tailed nonparametric Mann Whitney test with Gaussian approximation and confidence level of 95 %.

SUPPORTING INFORMATION

Supporting Information Available: Supplemental Figures and Tables are available free of charge via the Internet at http://pubs.acs.org.

ACKNOWLEDGMENTS

We would like to thank R. Allen, J. Fox, and D. Nelson at the Oregon Translational Research and Development Institute for use of their facility for and expert technical advice. We also wish to thank A. Nilsen at the OHSU Medicinal Chemistry Core and D. Koop at the OHSU Bioanalytical Shared Resource/ Pharmacokinetics Core for their chemical expertise and help in moving this project forward. Additional thanks go to C. Rizzo, Vanderbilt University for providing the TAMRA-conjugated oligodeoxynucleotides. This work was supported by funds from the Oregon Translational Research and Development Institute, the National Cancer Institute (award # P01 CA160032), the National Institute of Environmental Health Sciences (award # T32 ES007060), and the Oregon Clinical and Translational Research Institute.

Certain commercial equipment or materials are identified in this paper in order to specify adequately the experimental procedure. Such identification does not imply recommendation or endorsement by the National Institute of Standards and Technology, nor does it imply that the materials or equipment identified are necessarily the best available for the purpose.

FIGURES and TABLES

5′TAMRA-TCA CC**X** TCG TAC GAC TC
3′BHQ2--AGT GG**N** AGC ATG CTG AG

Enzyme	X=	N=
OGG1	8-oxo-Gua	C
Fpg	8-oxo-Gua	C
NEIL1	Sp/Gh	T
NTH1	ThyGly	A
Udg	U	C or A

Figure 1. Oligodeoxynucleotide sequences and position of lesions used for multiple DNA glycosylases. Enzymes used were OGG1, Fpg, NEIL1, NTH1, and uracil-DNA glycosylase (Udg). Lesions analyzed were 8-oxo-Gua, Sp/Gh, ThyGly, and uracil (U).

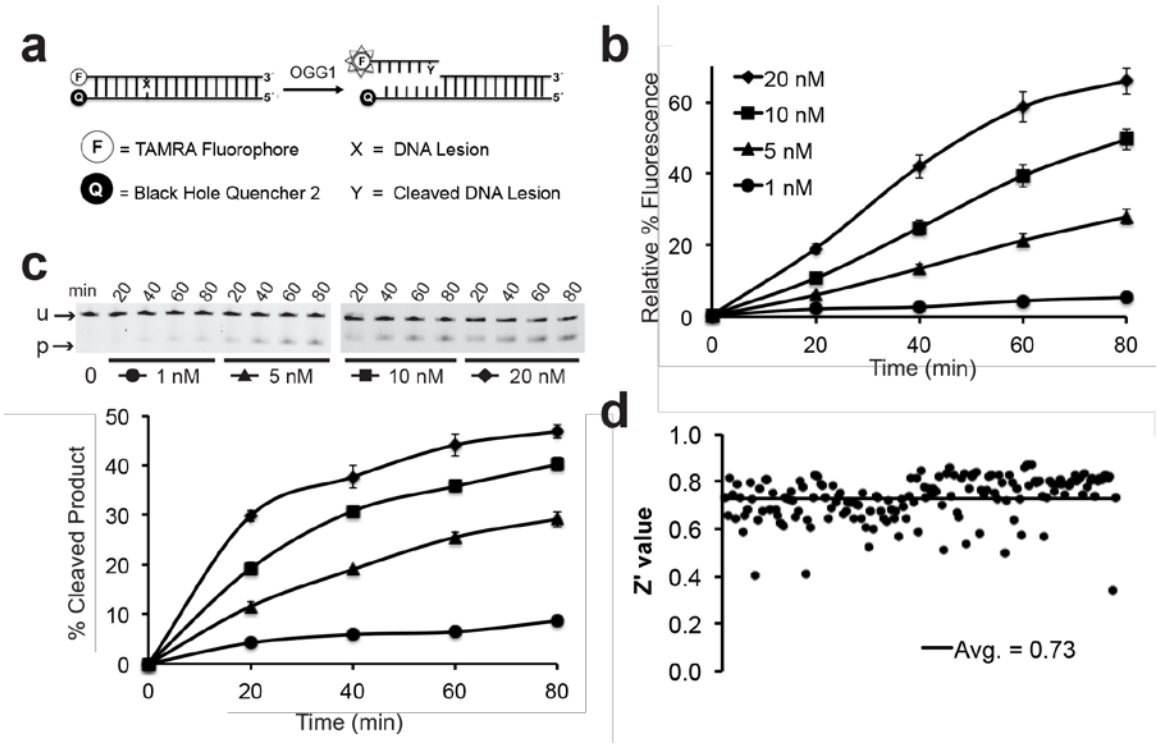

Figure 2. Overview of screening assay for OGG1 inhibitors. a) Schematic of the fluorescence-based OGG1 inhibitor assay used for the inhibitor screen. Image adapted from.[40] b and c) OGG1 dose (1-20 nM) and kinetic data for the fluorescence-based (b) and the gel-based (c) assays showing similar kinetics. Relative percent fluorescence equals the percent fluorescence in the experimental well compared to a well containing only the TAMRA strand of the substrate. Percent cleaved product equals the cleaved product (p) / (uncleaved substrate (u) + p). Data points equal the mean of three independent experiments. The uncertainties are standard deviations. d) Z' values for each of the 156 plates screened for OGG1 inhibition. Z´ values were calculated using fluorescence values from no inhibitor and no enzyme control wells on each plate.

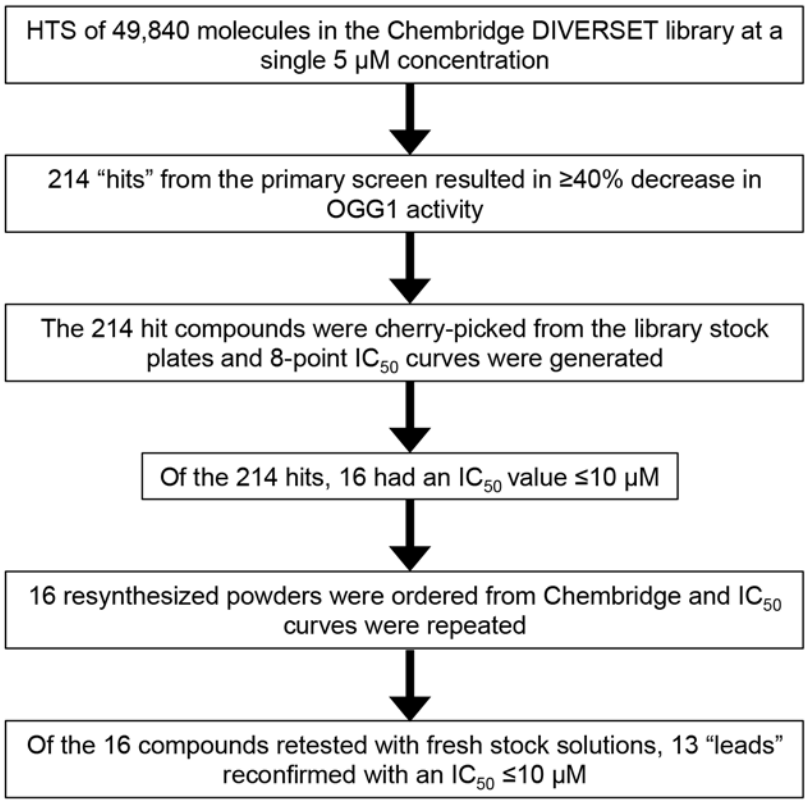

Figure 3. Diagram of lead compound identification.

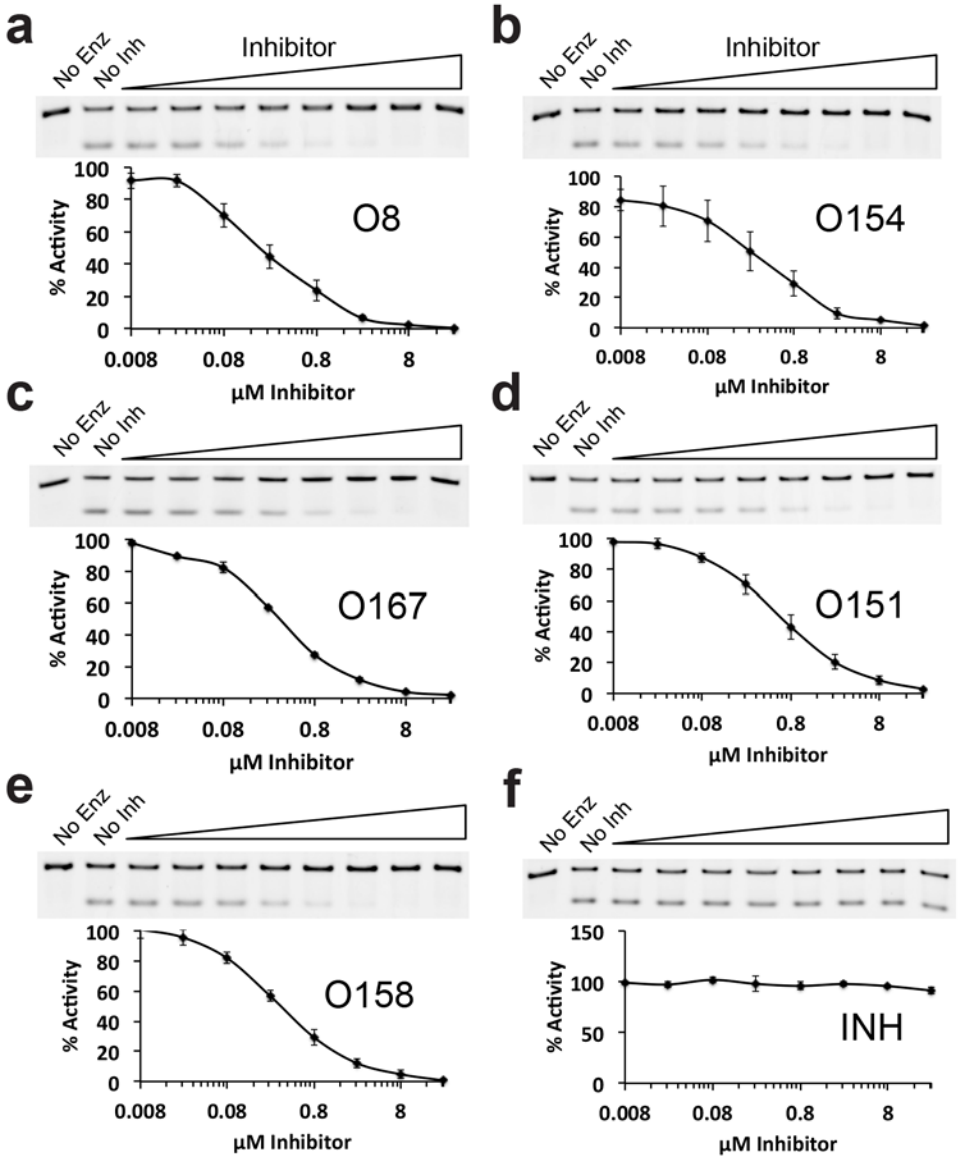

Figure 4. Gel-based OGG1 activity assay. 8-oxo-Gua–containing substrate was incubated without OGG1 (No Enz), with OGG1 (No Inh), or with OGG1 + 8 different concentrations (25, 8, 2.5, 0.8, 0.25, 0.08, 0.025, 0.008 µM) of inhibitors O8 (a), O154 (b), O167 (c), O151 (d), or O158 (e). The experiment was also conducted with the non-inhibitor INH (f). The top band in each gel corresponds to uncleaved substrate and the bottom band is cleaved product. The Y-axis on each graph

equals the percent substrate cleavage compared to the no inhibitor control (% Activity). Data points equal the mean of three independent experiments. The uncertainties are standard deviations. IC_{50} values calculated from these gels are listed in Table 1.

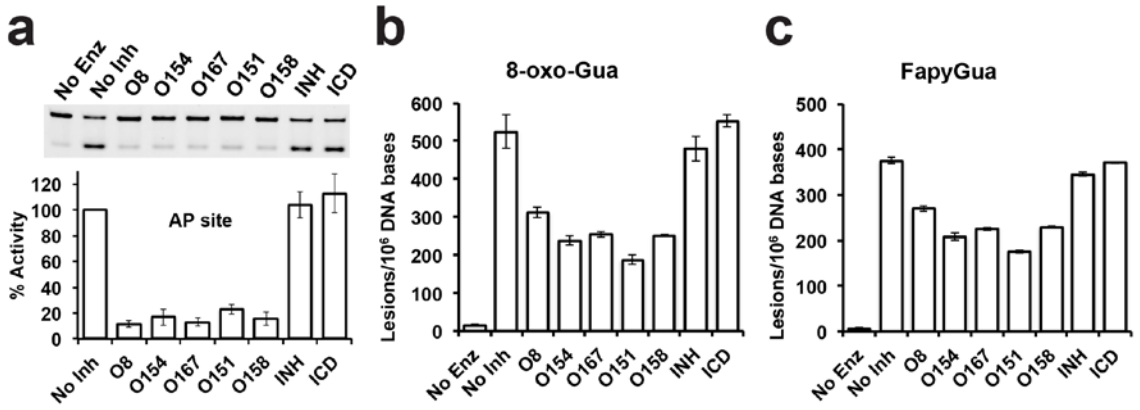

Figure 5. Inhibition of the glycosylase and lyase activities of OGG1. a) OGG1 lyase activity on a substrate containing an AP site. The substrate was incubated without OGG1 (No Enz), with OGG1 (No Inh), or with OGG1 + 10 μM compound. The top band in each gel corresponds to uncleaved substrate and the bottom band is cleaved product. Mean percent cleavage compared to the no inhibitor control (% Activity) was plotted for three independent experiments. The uncertainties are standard deviations. b and c) OGG1 glycosylase activity measured on irradiated calf thymus DNA. The number of excised 8-oxo-Gua (b) and FapyGua (c) per 10^6 DNA bases was measured by GC-MS/MS. Graph plots equal the mean of three independent experiments. The uncertainties are standard deviations.

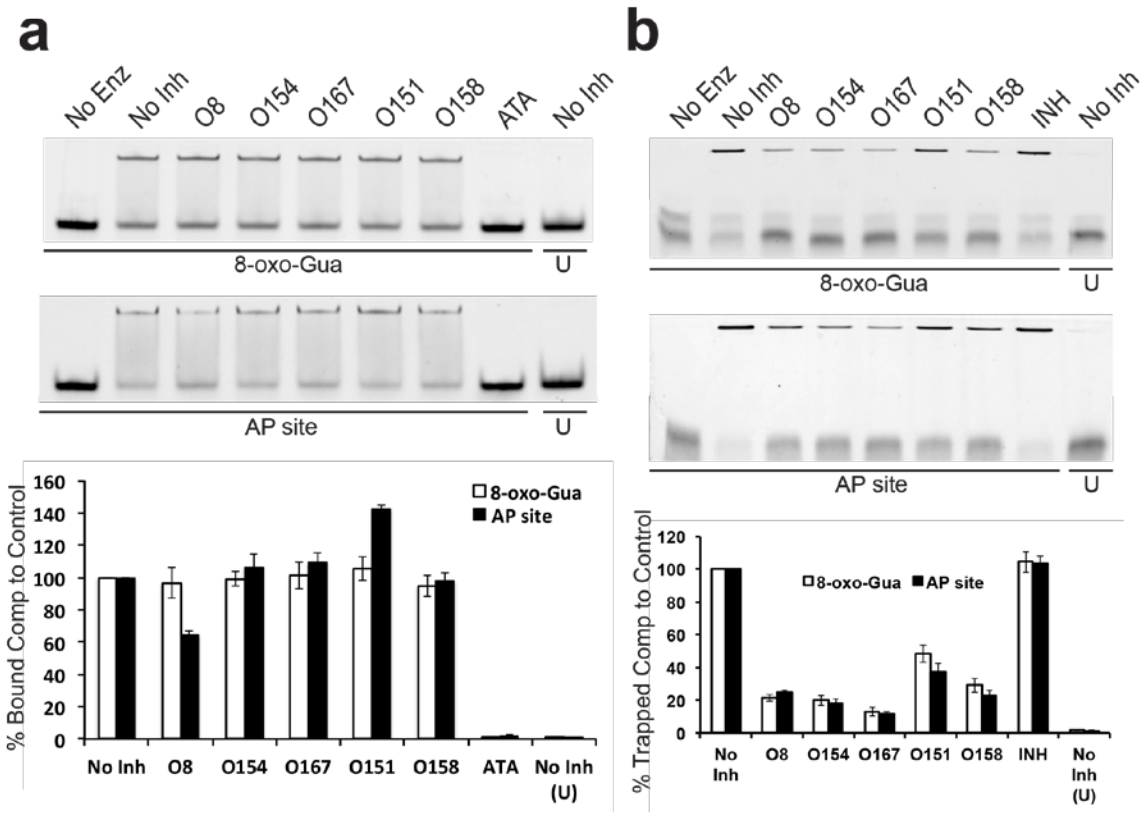

Figure 6. Mechanism of action of OGG1 inhibition. a) EMSA of OGG1 bound to various DNA substrates. OGG1 was incubated with 8-oxo-Gua- (top gel), AP site- (bottom gel) or U-containing (last lane in each gel) substrates with or without 50 μM inhibitor or aurintricarboxylic acid (ATA). Reactions were carried out at 4 °C for 5 min, conditions that were not permissive for OGG1 catalysis (data not shown). Top band in each gel corresponds to OGG1 bound to substrate and the bottom band is unbound substrate. Bands were quantified in each gel and the percent bound compared to the no inhibitor control was plotted for each compound. Graph plots equal the mean of three independent experiments. The uncertainties are standard deviations. b) Sodium cyanoborohydride trapping of OGG1 and substrate. OGG1 was incubated with 8-oxo-Gua– (top gel), AP site– (bottom gel) or U-containing (last lane in each gel) substrates with or without 10 μM inhibitor or

INH. Reactions were performed in the presence of 1 mM $NaBH_3CN$. Top band in each gel corresponds to OGG1 trapped to substrate and the bottom band is untrapped substrate. Bands were quantified in each gel and the percent trapped compared to the no inhibitor control was plotted for each compound. Graph plots equal the mean of three independent experiments. The uncertainties are standard deviations.

ID	Structure	IC_{50} (μM) gel	IC_{50} (μM) fluorescence	(% activity with 50 μM inhibitor)		
		OGG1		NEIL1	NTH1	Fpg
O8	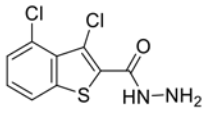	0.22 ± 0.08	0.35 ± 0.05	84.56%	63.09%	91.74%
O154	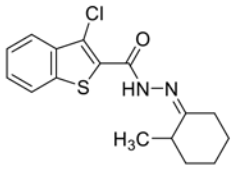	0.27 ± 0.15	0.37 ± 0.02	82.27%	94.85%	87.31%
O167	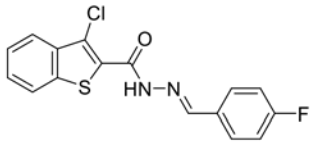	0.33 ± 0.02	0.42 ± 0.09	86.69%	89.21%	81.69%
O151	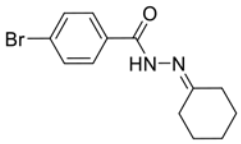	0.63 ± 0.18	0.61 ± 0.11	97.63%	84.47%	91.70%
O158	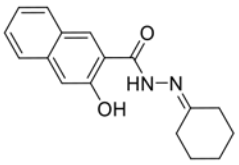	0.34 ± 0.04	0.29 ± 0.02	87.42%	83.02%	77.02%
Isoniazid (INH)	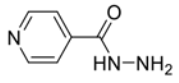	>50	>50	80.64%	97.95%	ND

Table 1. Inhibitor structures and ability to inhibit different DNA glycosylases. The first column contains the five most potent OGG1 inhibitors identified by our screen and one non-inhibitor (isoniazid, INH) with corresponding structures. The second column denotes the mean IC_{50} values from three independent experiments for the gel-based or fluorescence-based OGG1 assays. The uncertainties are standard

deviations. The third column indicates the percent activity of NEIL1, NTH1 or Fpg in the presence of 50 μM inhibitor compared to the no inhibitor control. ND = not determined.

REFERENCES

1. Dizdaroglu, M. (2015) Oxidatively induced DNA damage and its repair in cancer. *Mutat. Res. Rev. Mutat. Res. 763*, 212-245.
2. Kaur, R., Kaur, J., Mahajan, J., Kumar, R., and Arora, S. (2014) Oxidative stress--implications, source and its prevention. *Environ. Sci. Pollut. Res. Int. 21*, 1599-1613.
3. Hazra, T. K., Das, A., Das, S., Choudhury, S., Kow, Y. W., and Roy, R. (2007) Oxidative DNA damage repair in mammalian cells: a new perspective. *DNA Repair 6*, 470-480.
4. Brooks, S. C., Adhikary, S., Rubinson, E. H., and Eichman, B. F. (2013) Recent advances in the structural mechanisms of DNA glycosylases. *Biochim. Biophys. Acta 1834*, 247-271.
5. Hegde, M. L., Hazra, T. K., and Mitra, S. (2008) Early steps in the DNA base excision/single-strand interruption repair pathway in mammalian cells. *Cell Res. 18*, 27-47.
6. Beard, W. A., Batra, V. K., and Wilson, S. H. (2010) DNA polymerase structure-based insight on the mutagenic properties of 8-oxoguanine. *Mutat. Res. 703*, 18-23.
7. Dherin, C., Radicella, J. P., Dizdaroglu, M., and Boiteux, S. (1999) Excision of oxidatively damaged DNA bases by the human alpha-hOgg1 protein and the polymorphic alpha-hOgg1(Ser326Cys) protein which is frequently found in human populations. *Nucleic Acids Res. 27*, 4001-4007.
8. Dalhus, B., Forsbring, M., Helle, I. H., Vik, E. S., Forstrom, R. J., Backe, P. H., Alseth, I., and Bjoras, M. (2011) Separation-of-function mutants unravel the dual-reaction mode of human 8-oxoguanine DNA glycosylase. *Structure 19*, 117-127.
9. Curtin, N. J. (2012) DNA repair dysregulation from cancer driver to therapeutic target. *Nat. Rev. Cancer 12*, 801-817.
10. Hosoya, N., and Miyagawa, K. (2014) Targeting DNA damage response in cancer therapy. *Cancer Sci. 105*, 370-388.
11. Tutt, A., Robson, M., Garber, J. E., Domchek, S. M., Audeh, M. W., Weitzel, J. N., Friedlander, M., Arun, B., Loman, N., Schmutzler, R. K., Wardley, A., Mitchell, G., Earl, H., Wickens, M., and Carmichael, J. (2010) Oral

poly(ADP-ribose) polymerase inhibitor olaparib in patients with BRCA1 or BRCA2 mutations and advanced breast cancer: a proof-of-concept trial. *Lancet 376*, 235-244.

12. Mendes-Pereira, A. M., Martin, S. A., Brough, R., McCarthy, A., Taylor, J. R., Kim, J. S., Waldman, T., Lord, C. J., and Ashworth, A. (2009) Synthetic lethal targeting of PTEN mutant cells with PARP inhibitors. *EMBO Mol. Med. 1*, 315-322.
13. Sultana, R., McNeill, D. R., Abbotts, R., Mohammed, M. Z., Zdzienicka, M. Z., Qutob, H., Seedhouse, C., Laughton, C. A., Fischer, P. M., Patel, P. M., Wilson, D. M., 3rd, and Madhusudan, S. (2012) Synthetic lethal targeting of DNA double-strand break repair deficient cells by human apurinic/apyrimidinic endonuclease inhibitors. *Int. J. Cancer 131*, 2433-2444.
14. Martin, S. A., McCabe, N., Mullarkey, M., Cummins, R., Burgess, D. J., Nakabeppu, Y., Oka, S., Kay, E., Lord, C. J., and Ashworth, A. (2010) DNA polymerases as potential therapeutic targets for cancers deficient in the DNA mismatch repair proteins MSH2 or MLH1. *Cancer Cell 17*, 235-248.
15. Jacob, S., and Praz, F. (2002) DNA mismatch repair defects: role in colorectal carcinogenesis. *Biochimie 84*, 27-47.
16. Fishel, M. L., and Kelley, M. R. (2007) The DNA base excision repair protein Ape1/Ref-1 as a therapeutic and chemopreventive target. *Mol. Aspects Med. 28*, 375-395.
17. Curtin, N. J. (2013) Inhibiting the DNA damage response as a therapeutic manoeuvre in cancer. *Br. J. Pharmacol. 169*, 1745-1765.
18. Jaiswal, A. S., Banerjee, S., Panda, H., Bulkin, C. D., Izumi, T., Sarkar, F. H., Ostrov, D. A., and Narayan, S. (2009) A novel inhibitor of DNA polymerase beta enhances the ability of temozolomide to impair the growth of colon cancer cells. *Mol. Cancer Res. 7*, 1973-1983.
19. Hyun, J. W., Cheon, G. J., Kim, H. S., Lee, Y. S., Choi, E. Y., Yoon, B. H., Kim, J. S., and Chung, M. H. (2002) Radiation sensitivity depends on OGG1 activity status in human leukemia cell lines. *Free Radical Biol. Med. 32*, 212-220.
20. Larsen, E., Reite, K., Nesse, G., Gran, C., Seeberg, E., and Klungland, A. (2006) Repair and mutagenesis at oxidized DNA lesions in the developing brain of wild-type and Ogg1$^{-/-}$ mice. *Oncogene 25*, 2425-2432.
21. Taricani, L., Shanahan, F., Pierce, R. H., Guzi, T. J., and Parry, D. (2010) Phenotypic enhancement of thymidylate synthetase pathway inhibitors following ablation of Neil1 DNA glycosylase/lyase. *Cell Cycle 9*, 4876-4883.
22. Dziaman, T., Ludwiczak, H., Ciesla, J. M., Banaszkiewicz, Z., Winczura, A., Chmielarczyk, M., Wisniewska, E., Marszalek, A., Tudek, B., and Olinski, R. (2014) PARP-1 expression is increased in colon adenoma and carcinoma and correlates with OGG1. *PLoS One 9*, e115558.
23. Alli, E., Sharma, V. B., Sunderesakumar, P., and Ford, J. M. (2009) Defective repair of oxidative dna damage in triple-negative breast cancer confers sensitivity to inhibition of poly(ADP-ribose) polymerase. *Cancer Res. 69*, 3589-3596.

24. Noren Hooten, N., Kompaniez, K., Barnes, J., Lohani, A., and Evans, M. K. (2011) Poly(ADP-ribose) polymerase 1 (PARP-1) binds to 8-oxoguanine-DNA glycosylase (OGG1). *J. Biol. Chem. 286*, 44679-44690.
25. Preston, T. J., Henderson, J. T., McCallum, G. P., and Wells, P. G. (2009) Base excision repair of reactive oxygen species-initiated 7,8-dihydro-8-oxo-2'-deoxyguanosine inhibits the cytotoxicity of platinum anticancer drugs. *Mol. Cancer Ther. 8*, 2015-2026.
26. Ramdzan, Z. M., Vadnais, C., Pal, R., Vandal, G., Cadieux, C., Leduy, L., Davoudi, S., Hulea, L., Yao, L., Karnezis, A. N., Paquet, M., Dankort, D., and Nepveu, A. (2014) RAS transformation requires CUX1-dependent repair of oxidative DNA damage. *PLoS Biol. 12*, e1001807.
27. Jaruga, P., Zastawny, T. H., Skokowski, J., Dizdaroglu, M., and Olinski, R. (1994) Oxidative DNA base damage and antioxidant enzyme activities in human lung cancer. *FEBS Letters 341*, 59-64.
28. Cooke, M. S., Olinski, R., and Evans, M. D. (2006) Does measurement of oxidative damage to DNA have clinical significance? *Clin. Chim. Acta 365*, 30-49.
29. Gad, H., Koolmeister, T., Jemth, A. S., Eshtad, S., Jacques, S. A., Strom, C. E., Svensson, L. M., Schultz, N., Lundback, T., Einarsdottir, B. O., Saleh, A., Gokturk, C., Baranczewski, P., Svensson, R., Berntsson, R. P., Gustafsson, R., Stromberg, K., Sanjiv, K., Jacques-Cordonnier, M. C., Desroses, M., Gustavsson, A. L., Olofsson, R., Johansson, F., Homan, E. J., Loseva, O., Brautigam, L., Johansson, L., Hoglund, A., Hagenkort, A., Pham, T., Altun, M., Gaugaz, F. Z., Vikingsson, S., Evers, B., Henriksson, M., Vallin, K. S., Wallner, O. A., Hammarstrom, L. G., Wiita, E., Almlof, I., Kalderen, C., Axelsson, H., Djureinovic, T., Puigvert, J. C., Haggblad, M., Jeppsson, F., Martens, U., Lundin, C., Lundgren, B., Granelli, I., Jensen, A. J., Artursson, P., Nilsson, J. A., Stenmark, P., Scobie, M., Berglund, U. W., and Helleday, T. (2014) MTH1 inhibition eradicates cancer by preventing sanitation of the dNTP pool. *Nature 508*, 215-221.
30. Huber, K. V., Salah, E., Radic, B., Gridling, M., Elkins, J. M., Stukalov, A., Jemth, A. S., Gokturk, C., Sanjiv, K., Stromberg, K., Pham, T., Berglund, U. W., Colinge, J., Bennett, K. L., Loizou, J. I., Helleday, T., Knapp, S., and Superti-Furga, G. (2014) Stereospecific targeting of MTH1 by (S)-crizotinib as an anticancer strategy. *Nature 508*, 222-227.
31. Ba, X., Aguilera-Aguirre, L., Sur, S., and Boldogh, I. (2015) 8-Oxoguanine DNA glycosylase-1-driven DNA base excision repair: role in asthma pathogenesis. *Curr. Opin. Allergy Clin. Immunol. 15*, 89-97.
32. Bacsi, A., Aguilera-Aguirre, L., Szczesny, B., Radak, Z., Hazra, T. K., Sur, S., Ba, X., and Boldogh, I. (2013) Down-regulation of 8-oxoguanine DNA glycosylase 1 expression in the airway epithelium ameliorates allergic lung inflammation. *DNA Repair 12*, 18-26.
33. Hajas, G., Bacsi, A., Aguilera-Aguirre, L., Hegde, M. L., Tapas, K. H., Sur, S., Radak, Z., Ba, X., and Boldogh, I. (2013) 8-Oxoguanine DNA glycosylase-1 links DNA repair to cellular signaling via the activation of the small GTPase Rac1. *Free Radical Biol. Med. 61C*, 384-394.

34. Li, G., Yuan, K., Yan, C., Fox, J., 3rd, Gaid, M., Breitwieser, W., Bansal, A. K., Zeng, H., Gao, H., and Wu, M. (2012) 8-Oxoguanine-DNA glycosylase 1 deficiency modifies allergic airway inflammation by regulating STAT6 and IL-4 in cells and in mice. *Free Radical Biol. Med. 52*, 392-401.
35. German, P., Szaniszlo, P., Hajas, G., Radak, Z., Bacsi, A., Hazra, T. K., Hegde, M. L., Ba, X., and Boldogh, I. (2013) Activation of cellular signaling by 8-oxoguanine DNA glycosylase-1-initiated DNA base excision repair. *DNA Repair 12*, 856-863.
36. Aguilera-Aguirre, L., Bacsi, A., Radak, Z., Hazra, T. K., Mitra, S., Sur, S., Brasier, A. R., Ba, X., and Boldogh, I. (2014) Innate inflammation induced by the 8-oxoguanine DNA glycosylase-1-KRAS-NF-kappaB pathway. *J. Immunol. 193*, 4643-4653.
37. Luo, J., Hosoki, K., Bacsi, A., Radak, Z., Hegde, M. L., Sur, S., Hazra, T. K., Brasier, A. R., Ba, X., and Boldogh, I. (2014) 8-Oxoguanine DNA glycosylase-1-mediated DNA repair is associated with Rho GTPase activation and alpha-smooth muscle actin polymerization. *Free Radical Biol. Med*. *73*, 430-438.
38. Ba, X., Bacsi, A., Luo, J., Aguilera-Aguirre, L., Zeng, X., Radak, Z., Brasier, A. R., and Boldogh, I. (2014) 8-oxoguanine DNA glycosylase-1 augments proinflammatory gene expression by facilitating the recruitment of site-specific transcription factors. *J. Immunol. 192*, 2384-2394.
39. Aguilera-Aguirre, L., Hosoki, K., Bacsi, A., Radak, Z., Wood, T. G., Widen, S. G., Sur, S., Ameredes, B. T., Saavedra-Molina, A., Brasier, A. R., Ba, X., and Boldogh, I. (2015) Whole transcriptome analysis reveals an 8-oxoguanine DNA glycosylase-1-driven DNA repair-dependent gene expression linked to essential biological processes. *Free Radical Biol. Med. 81*, 107-118.
40. Jacobs, A. C., Calkins, M. J., Jadhav, A., Dorjsuren, D., Maloney, D., Simeonov, A., Jaruga, P., Dizdaroglu, M., McCullough, A. K., and Lloyd, R. S. (2013) Inhibition of DNA glycosylases via small molecule purine analogs. *PLoS One 8*, e81667.
41. Hazra, T. K., Izumi, T., Boldogh, I., Imhoff, B., Kow, Y. W., Jaruga, P., Dizdaroglu, M., and Mitra, S. (2002) Identification and characterization of a human DNA glycosylase for repair of modified bases in oxidatively damaged DNA. *Proc. Natl. Acad. Sci. U.S.A. 99*, 3523-3528.
42. Roy, L. M., Jaruga, P., Wood, T. G., McCullough, A. K., Dizdaroglu, M., and Lloyd, R. S. (2007) Human polymorphic variants of the NEIL1 DNA glycosylase. *J. Biol. Chem. 282*, 15790-15798.
43. Jaruga, P., Birincioglu, M., Rosenquist, T. A., and Dizdaroglu, M. (2004) Mouse NEIL1 protein is specific for excision of 2,6-diamino-4-hydroxy-5-formamidopyrimidine and 4,6-diamino-5-formamidopyrimidine from oxidatively damaged DNA. *Biochemistry 43*, 15909-15914.
44. Hu, J., de Souza-Pinto, N. C., Haraguchi, K., Hogue, B. A., Jaruga, P., Greenberg, M. M., Dizdaroglu, M., and Bohr, V. A. (2005) Repair of formamidopyrimidines in DNA involves different glycosylases: role of the OGG1, NTH1, and NEIL1 enzymes. *J. Biol. Chem. 280*, 40544-40551.

45. Boiteux, S., Gajewski, E., Laval, J., and Dizdaroglu, M. (1992) Substrate specificity of the Escherichia coli Fpg protein (formamidopyrimidine-DNA glycosylase): excision of purine lesions in DNA produced by ionizing radiation or photosensitization. *Biochemistry 31*, 106-110.
46. Melton, D., Lewis, C. D., Price, N. E., and Gates, K. S. (2014) Covalent adduct formation between the antihypertensive drug hydralazine and abasic sites in double- and single-stranded DNA. *Chem. Res. Toxicol. 27*, 2113-2118.
47. Gonzalez, R. G., Haxo, R. S., and Schleich, T. (1980) Mechanism of action of polymeric aurintricarboxylic acid, a potent inhibitor of protein--nucleic acid interactions. *Biochemistry 19*, 4299-4303.
48. Kurtz, A. J., Dodson, M. L., and Lloyd, R. S. (2002) Evidence for multiple imino intermediates and identification of reactive nucleophiles in peptide-catalyzed beta-elimination at abasic sites. *Biochemistry 41*, 7054-7064.
49. Hill, J. W., and Evans, M. K. (2006) Dimerization and opposite base-dependent catalytic impairment of polymorphic S326C OGG1 glycosylase. *Nucleic Acids Res. 34*, 1620-1632.
50. Biela, A., Coste, F., Culard, F., Guerin, M., Goffinont, S., Gasteiger, K., Ciesla, J., Winczura, A., Kazimierczuk, Z., Gasparutto, D., Carell, T., Tudek, B., and Castaing, B. (2014) Zinc finger oxidation of Fpg/Nei DNA glycosylases by 2-thioxanthine: biochemical and X-ray structural characterization. *Nucleic Acids Res. 42*, 10748-10761.
51. Jaruga, P., Kirkali, G., and Dizdaroglu, M. (2008) Measurement of formamidopyrimidines in DNA. *Free Radical Biol. Med. 45*, 1601-1609.
52. Reddy, P. T., Jaruga, P., Kirkali, G., Tuna, G., Nelson, B. C., and Dizdaroglu, M. (2013) Identification and quantification of human DNA repair protein NEIL1 by liquid chromatography/isotope-dilution tandem mass spectrometry. *J. Proteome Res. 12*, 1049-1061.

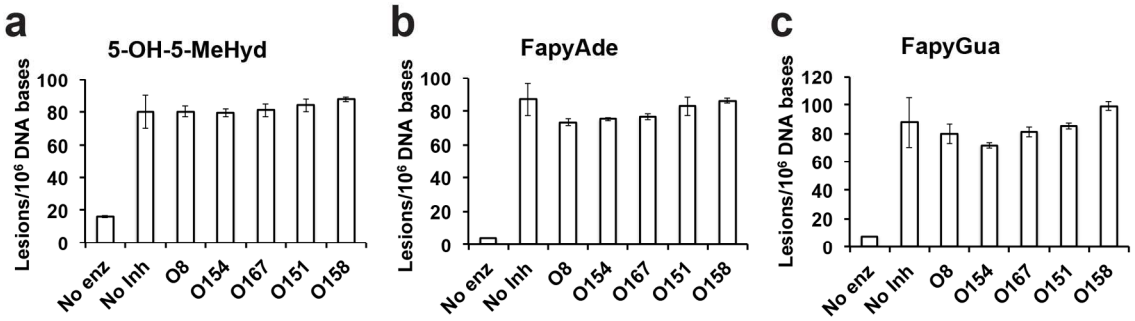

Supplemental Figure 1. Lack of inhibition of NEIL1 glycosylase activity. NEIL1 glycosylase activity was measured on γ-irradiated calf thymus DNA. The number of excised 5-OH-5-MeHyd (a), FapyAde (b), FapyGua (c) lesions per 10^6 bases were measured by GC-MS/MS. Graph plots equal the mean of three independent experiments. The uncertainties are standard deviations.

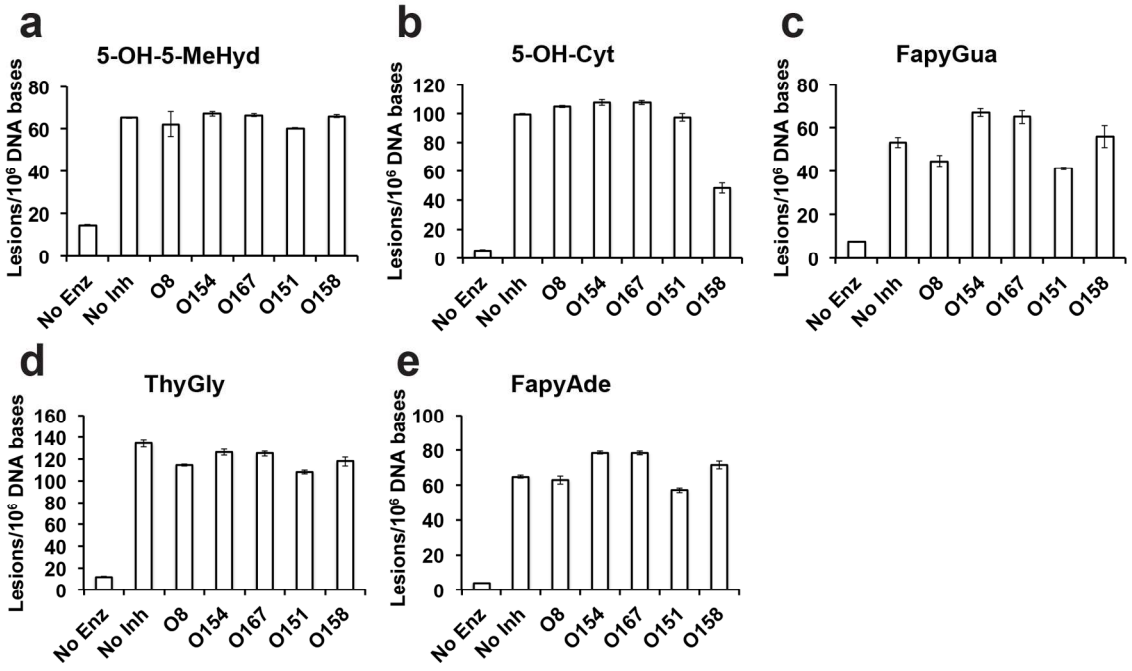

Supplemental Figure 2. Lack of inhibition of NTH1 glycosylase activity. NTH1 glycosylase activity was measured on γ-irradiated calf thymus DNA. The number of excised 5-OH-5-MeHyd (a), 5-OH-Cyt (b), FapyGua (c), ThyGly (d), or FapyAde (e) lesions per 10^6 bases were measured by GC-MS/MS. Graph plots equal the mean of three independent experiments. The uncertainties are standard deviations.

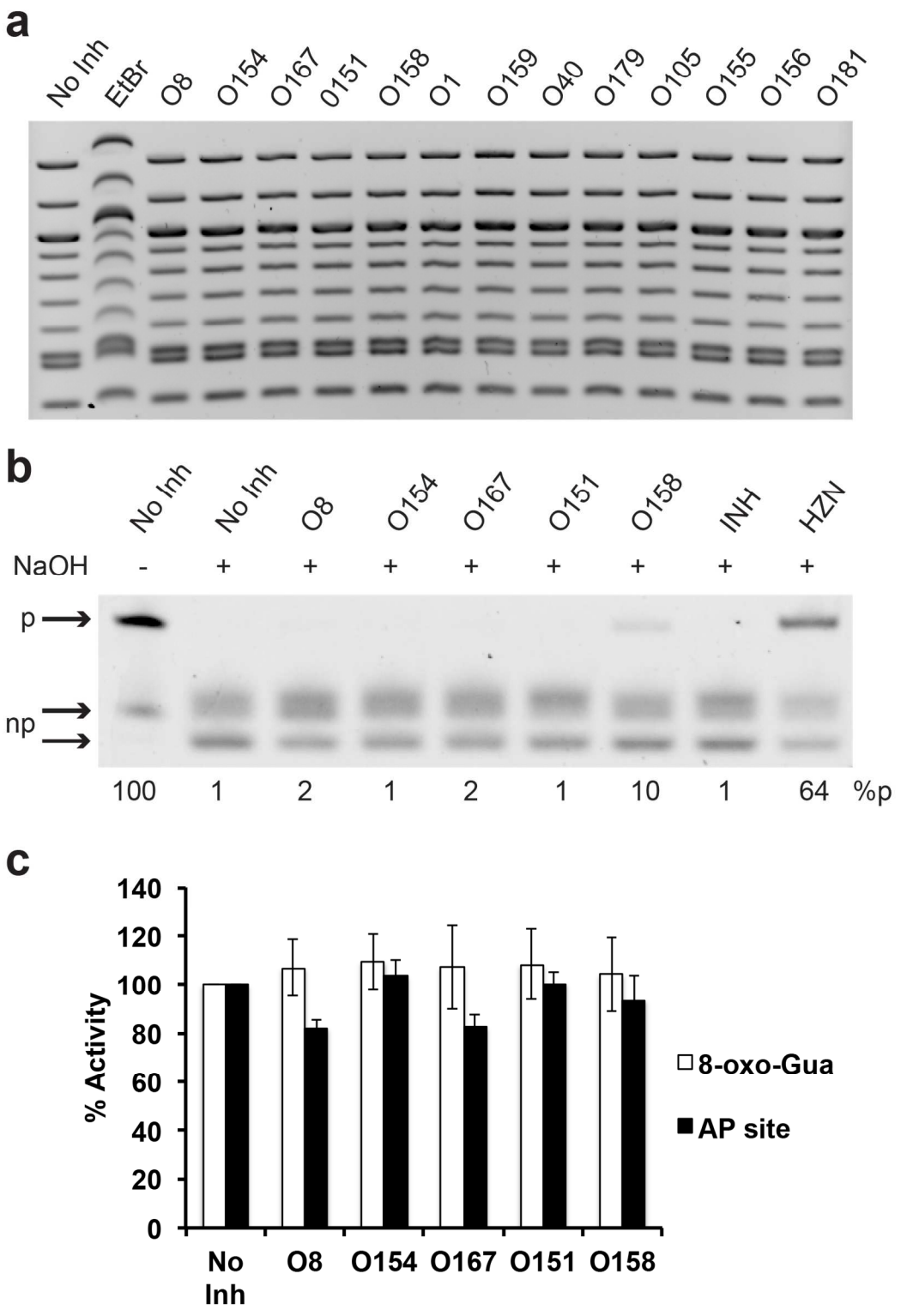

Supplemental Figure 3. OGG1 inhibitors do not alter the structure of DNA. a) 500 ng DNA ladder was incubated with buffer (No Inh), 50 μM EtBr or 50 μM

OGG1 inhibitor for 30 min at RT, run on a gel and post-stained with EtBr to visualize bands. b) Alkaline cleavage protection assay. 25 nM AP-site substrate was incubated with 50 μM OGG1 inhibitor, isoniazid (INH), hydralazine (HZN) or buffer (No Inh) at 37 °C for 30 min. NaOH was then added to the reaction to a final concentration of 0.15M and samples were left at 37 °C for an additional 1.5 hours. Samples were mixed 1:1 with formamide and run on a 15% denaturing gel. Top band in each gel corresponds to full length AP site substrate and the bottom band(s) correspond to substrate cleaved at the AP site. Percent protected (%p) values at the bottom of the gel were calculated for each lane and normalized to the no NaOH control. c) Substrate pre-incubation with inhibitors. 25 nM 8-oxo-Gua or AP site substrate was incubated with 20 μM OGG1 inhibitor at 37 °C for 30 min followed by the addition of 0.011 Units of Fpg. Fluorescence was analyzed at 10 min. Percent activity equals the background-subtracted fluorescence in the experimental well compared to the same value in the no inhibitor control. Graph plots equal the mean of three independent experiments. The uncertainties are standard deviations.

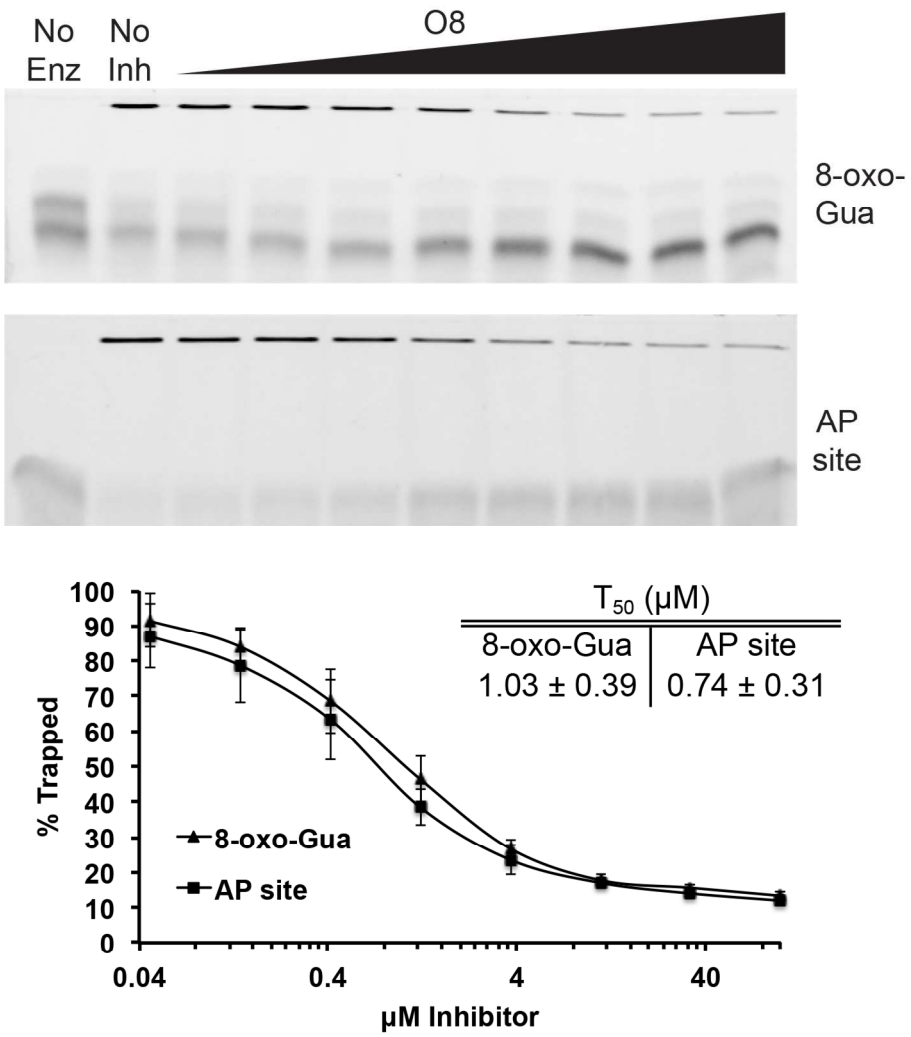

Supplemental Figure 4. Dose response for O8 trapping. Sodium cyanoborohydride trapping experiment of OGG1 and substrate. 50 nM OGG1 was incubated with 25 nM 8-oxo-Gua- (top gel) or AP site-containing (bottom gel) substrate with or without 8 different concentrations of O8 inhibitor (0.05, 0.14, 0.4, 1.2, 3.7, 11, 33, 100 μM). Reactions were performed in the presence of 1 mM $NaBH_3CN$. Top band in each gel corresponds to OGG1 trapped to substrate and the bottom band is untrapped substrate. Bands were quantified in each gel and the percent trapped compared to the no inhibitor control (% Trapped) was

plotted for each compound. Graph plots equal the mean of three independent experiments. The uncertainties are standard deviations. Mean T_{50} values in μM ± std. dev. were calculated as described in the Methods section.

Identified in the Screen						Additional Compounds					
ID	Structure	IC_{50} (μM) fluorescence	(% activity with 50 μM inhibitor)			ID	Structure	IC_{50} (μM) fluorescence	(% activity with 50 μM inhibitor)		
		OGG1	NEIL1	NTH1	Fpg			OGG1	NEIL1	NTH1	Fpg
O1	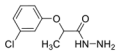	3.38 ± 0.44	95.31%	100.21%	90.75%	**Isocarboxazid (ICD)**	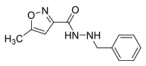	>50	93.27%	104.61%	ND
O159	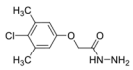	1.53 ± 0.14	83.74%	75.07%	94.97%	**Nialamide**	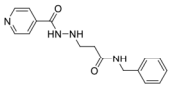	>50	96.40%	108.35%	ND
O40	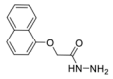	1.56 ± 0.2	78.68%	53.61%	88.54%	**O8-Cl**	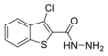	0.30 ± 0.04	ND	ND	ND
O179	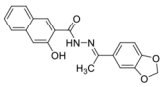	7.17 ± 0.39	51.95%	72.98%	ND	**O151-Hy**	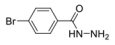	0.39 ± 0.04	ND	ND	ND
O181	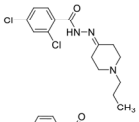	4.56 ± 1.29	91.25%	96.14%	ND	**O151-Am**		>50	ND	ND	ND
O155	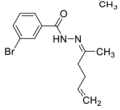	3.78 ± 0.08	93.51%	90.57%	78.81%	**Hydralazine (HZN)**		>50	ND	ND	ND
O156	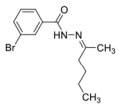	2.13 ± 0.29	100.60%	92.63%	90.87%						
O105	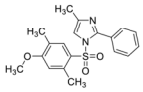	4.15 ± 1.1	100.02%	108.62%	ND						

Supplemental Table 1. Remaining OGG1 inhibitors and additional compounds screened. The first column in each section contains the remaining eight OGG1 inhibitors identified in the screen and additional compounds that were screened for OGG1 inhibition along with corresponding structures. The second column denotes the mean IC_{50} values from three independent experiments ± std. dev. for the fluorescence-based OGG1 assay. The third column indicates the percent activity of NEIL1, NTH1 or Fpg in the presence of 50 μM inhibitor compared to the no inhibitor control. ND = not determined.